Computers and Concrete, *Vol. 13, No. 3 (2014) 325-342*
DOI: http://dx.doi.org/10.12989/cac.2014.13.3.325

Producing synthetic lightweight aggregates by treating waste TFT-LCD glass powder and reservoir sediments

Chao-Wei Tang*

Department of Civil Engineering and Geomatics, Cheng Shiu University, 840 Chengcing Road, Niaosong District, Kaohsiung City 833, Taiwan

(*Received August 7, 2013, Revised November 7, 2013, Accepted November 29 2013*)

Abstract. The use of lightweight aggregate (LWA) instead of ordinary aggregate may make lightweight aggregate concrete, which possesses many advantages such as lightweight, lower thermal conductivity, and better fire and seismic resistance. Recently the developments of LWA have been focused on using industrial wastes as raw materials to reduce the use of limited natural resources. In view of this, the intent of this study was to apply Taguchi optimization technique in determining process condition for producing synthetic LWA by incorporating waste thin film transition liquid crystal displays (TFT-LCD) glass powder with reservoir sediments. In the study the waste TFT-LCD glass cullet was used as an additive. It was incorporated with reservoir sediments to produce LWA. Taguchi method with an orthogonal array $L_{16}(4^5)$ and five controllable 4-level factors (i.e., cullet content, preheat temperature, preheat time, sintering temperature, and sintering time) was adopted. Then, in order to optimize the selected parameters, the analysis of variance method was used to explore the effects of the experimental factors on the performances (particle density, water absorption, bloating ratio, and loss of ignition) of the produced LWA. The results showed that it is possible to produce high performance LWA by incorporating waste TFT-LCD glass cullet with reservoir sediments. Moreover, Taguchi method is a promising approach for optimizing process condition of synthetic LWA using recycled glass cullet and reservoir sediments and it significantly reduces the number of tests.

Keywords: lightweight aggregate; cullet; taguchi experimental design method

1. Introduction

Lightweight aggregate (LWA) is the generic name of a group of aggregates having a relative density lower than normal density aggregates (natural sand, gravel, and crushed stone), sometimes and is referred to as low-density aggregate (Somayaji 2001, Chandra and Berntsson 2002, Mindess *et al*. 2003, Metha and Monteiro 2006). LWA used to decrease the unit weight of concrete, thereby reducing the structural load. In addition, LWA may be found in other applications including concrete masonry, asphalt pavement, geotechnical fill, horticultural and soil amendment, concrete wall board, roof tile, refractory products, filter media, and high-performance concrete (Doel 2007).

LWA can be grouped into two distinct categories; natural LWA and synthetic LWA (Somayaji 2001, Chandra and Berntsson 2002, Mindess *et al*. 2003, Metha and Monteiro 2006). Natural

*Corresponding author, Professor, E-mail: tangcw@csu.edu.tw

http://www.techno-press.org/?journal=cac&subpage=8 ISSN: 1598-8198 (Print), 1598-818X (Online)

LWA consist of particles derived from natural rocks and are ready to use only with mechanical treatment, i.e., crushing and sieving. While synthetic LWA is mainly produced by thermal treatment from either naturally occurring materials or from industrial by-products, waste materials, potential raw materials, etc. Thermal expansion in the raw materials used for producing synthetic LWA is the most significant condition. Generally speaking, expansion takes place when the material is heated to fusion temperature at which point pyro-plasticity of the material occurs simultaneously with the formation of gas. Therefore, there are two necessary requirements for the raw material to form and expand (Riley 1951). The first requirement is glassed phase formation under high temperature with enough material adhesion to contain the expanding gases. The second requirement is that material components must exist that can discharge the gas when the glassed phase is formed.

Over the last few decades, the development of LWA has been focused on the use of industrial by-products, waste materials, or sedimentary as raw materials to limit the use of irreplaceable natural resources and to still satisfy the growing demand for aggregates (Chandra and Berntsson 2002). Moreover, the use of these artificial low-density aggregates can achieve not only technical benefits but economic and ecological benefits as well.

Taiwan is a leading country in thin film transition liquid crystal displays (TFT-LCD) manufacturing. According to a July 2008 statistic from the Department of Waste Management under the Taiwan Environmental Protection Administration (EPA), the amount of waste TFT-LCD glass produced in Taiwan has increased very rapidly in recent years. Therefore, there is an urgent need to develop novel reuse applications for waste TFT-LCD glass in Taiwan.

There are numerous studies on production of LWA using incinerator bottom ashes, fly ashes, sewage sludge, reservoir sediment, etc. (Wainwright and Cresswell 2001, Ducman *et al*. 2002, Cheeseman *et al*. 2005, Cheeseman and Virdi 2005, Chiou *et al*. 2006, Mun 2007, Kayali 2008, Qiao *et al*. 2008, Muellera *et al*. 2008, Chen *et al*. 2010, Kourti and Cheeseman 2010, Tang *et al*. 2011, Chen *et al*. 2012, Bajare *et al*. 2012, Huang and Wang 2013, Liao *et al*. 2013, Shon *et al*. 2013, Yaghi and Hartikainen 2013, Donatello and Cheeseman 2013, Bernhardt *et al*. 2013, Chung *et al*. 2013). However, there are relatively few published studies on the use of waste thin film transition liquid crystal displays (TFT-LCD) glass in manufacturing LWA. In view of increasing concerns over non-renewable resource depletion and waste management, this research aimed at conducting an investigation on the development of LWA by incorporating waste TFT-LCD glass cullet with reservoir sediments. The investigation was performed in a laboratory scale to assess the effects of the composition and the firing conditions on the properties of the resulting aggregate. The research findings for this new type of construction material, reported here, should be beneficial to the safe treatment and disposal of waste TFT-LCD glass and reservoir sediments.

2. Experimental design and data analysis

2.1 Materials

The main materials used in the study included ground waste TFT-LCD glass and reservoir sediments. The cullet was collected from a TFT-LCD panel factory located in southern Taiwan. The reservoir sediments were collected from the Shihmen Reservoir located in northern Taiwan. From the theoretical aspect of sintering, the driving force required to reach the sintered state is proportional to the surface area of the as powder particles (German 1996). Therefore, the

sedimentation analysis (i.e., hydrometer analysis) was conducted to establish particle size distribution characteristics for the ashes with particles less than 75 μm in size. Then the complete particle size distributions of selected materials were done by combining the results of sieve analysis and hydrometer analysis, as shown in Fig. 1. As can be observed from Fig. 1 that the D_{50} particle sizes for the reservoir sediments was 0.007 mm, while the cullet had larger portion of coarse particles. This indicates that the cullet should be milled prior to mixing with reservoir sediments to satisfy the requirements for graining and sintering.

Table 1 presents the results of physical tests of the materials used in the study. As can be seen from Table 1, the specific gravity for the cullet and reservoir sediments were 2.67 and 2.75, respectively. In addition, the plasticity indexes (PI) for the reservoir sediments was 10%, which are inorganic clays according to the Unified Soil Classification System. This indicates the sediments had a proper plasticity. By contrast, the cullet had poor plasticity. In general, the higher the PI, the more plastic the material is, and thus making the graining process much easier. This is one of the major reasons that a large proportion of the designed mixture was the reservoir sediments in the study. In other words, the waste TFT-LCD glass cullet was used as an additive and was incorporated into reservoir sediments to produce LWA.

On the other hand, the chemical composition of the raw materials used is presented in Table 2. The TFT-LCD glass cullet has a high SiO_2 content (67.9%) and low concentrations of fluxing (Fe_2O_3 + CaO + MgO + K_2O + Na_2O, 10.1%). While the reservoir sediments shows a lower SiO_2 content (53.4%) and high values of fluxing (21.8%). The main components (SiO_2 and Al_2O_3) would ensure the development of a highly viscous liquid phase at high temperature, which could entrap the gases. The fluxing would influence the softening and melting temperatures of aggregates (Riley 1951). Overall, the analysis results fell in the area of the expandable region of the ternary (SiO_2/Al_2O_3/fluxing) diagram produced by Riley (See Fig. 2). Based on these observations and analysis, the cullet and the sediments are feasible for sintering LWA.

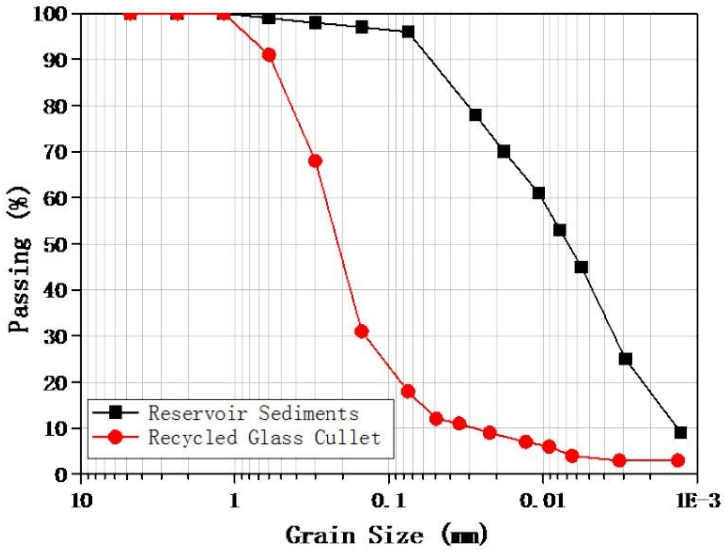

Fig. 1 Grain size distributions of cullet and reservoir sediments

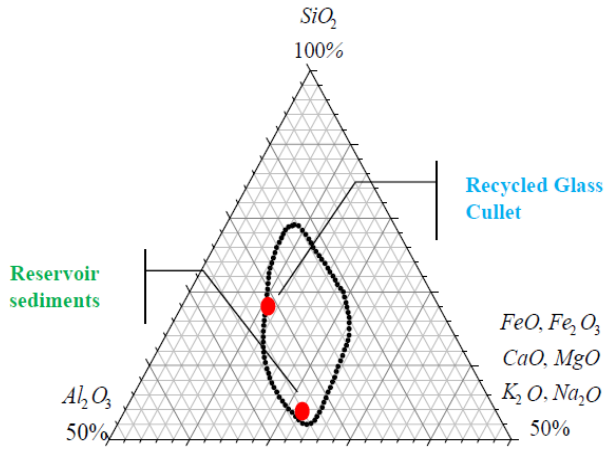

Fig. 2 Ternary diagram of cullet and reservoir sediments

Table 1 Physical test results of cullet and reservoir sediments

Sample	Specific gravity	PI (%)	Ingredients (% wt.)			
			Gravels (＞4.75 mm)	Sands (4.75-0.075 mm)	Silts (0.075-0.005 mm)	Clays (＜0.005 mm)
Cullet	2.67	NP	0	82	14	4
Sediments	2.75	10	0	4	54	42

Table 2 Chemical composition of cullet and reservoir sediments

Sample	Chemical compositions (wt.%)									
	SiO_2	Al_2O_3	Fe_2O_3	CaO	MgO	K_2O	Na_2O	OS	LOI	Total
Cullet	67.9	21.9	0.8	6.0	3.3	-	-	0.1	3.5	100
Sediments	53.4	23.8	10.9	1.8	2.5	5.1	1.5	1.0	2.9	100

Notes: LOI=Loss on ignition; OS=Organic substance content.

2.2 Design of experiment

Taguchi method, proposed by Dr. Genichi Taguchi, was developed based on the concept of the orthogonal array (OA), which can effectively reduce the number of tests required in a design procedure (Taguchi 1987, Roy 1990, Roy 2001, Taguchi 2005). Therefore, Taguchi method was used for designing the experiment in the study. The selected process parameters (i.e., cullet content, preheat temperature, preheat time, sintering temperature, and sintering time) and their levels are given in Table 3. The interaction between the process parameters is neglected. In addition, performance parameters (i.e., particle density, water absorption, bloating ratio, and loss of ignition) are also given in Table 3. Then, an $L_{16}(4^5)$ OA and five controllable 4-level factors was adopted

Table 3 Process parameters and design levels

Parameter (Experimental control factor)	Levels of parameter				Performance parameter value
	1	2	3	4	
Cullet content, A (%)	10	20	30	40	1. Particle density (g/cm^3) 2. Water absorption (%) 3. Bloating ratio (%) 4. Loss of ignition (%)
Preheat temperature, B (°C)	300	500	700	900	
Preheat time, C (min.)	7.5	15	22.5	30	
Sintering temperature, D (°C)	1100	1125	1150	1175	
Sintering time, E (min.)	10	15	20	25	

Table 4 Orthogonal array for $L_{16}(4^5)$

Experiment Number	Parameter (level)				
	A	B	C	D	E
G1	10(1)	300(1)	7.5(1)	1100(1)	10(1)
G2	10(1)	500(2)	15(2)	1125(2)	15(2)
G3	10(1)	700(3)	22.5(3)	1150(3)	20(3)
G4	10(1)	900(4)	30(4)	1175(4)	25(4)
G5	20(2)	300(1)	15(2)	1150(3)	25(4)
G6	20(2)	500(2)	7.5(1)	1175(4)	20(3)
G7	20(2)	700(3)	30(4)	1100(1)	15(2)
G8	20(2)	900(4)	22.5(3)	1125(2)	10(1)
G9	30(3)	300(1)	22.5(3)	1175(4)	15(2)
G10	30(3)	500(2)	30(4)	1150(3)	10(1)
G11	30(3)	700(3)	7.5(1)	1125(2)	25(4)
G12	30(3)	900(4)	15(2)	1100(1)	20(3)
G13	40(4)	300(1)	30(4)	1125(2)	20(3)
G14	40(4)	500(2)	22.5(3)	1100(1)	25(4)
G15	40(4)	700(3)	15(2)	1175(4)	10(1)
G16	40(4)	900(4)	7.5(1)	1150(3)	15(2)

(See Table 4). In order to optimize the selected parameters, the range analysis and analysis of variance the mathematical statistics were used to explore the effects of the experimental factors on the performances of the produced lightweight aggregates.

2.3 Preparation of aggregate pellets and aggregate firing

Samples of raw materials were dried prior to use in the graining process. Then each sample was crushed and milled using a Leading-Coming-Air Type crushing machine. According to the designed proportions (Table 4), the resulting fine powders were thoroughly mixed to ensure homogeneity. Then a controlled amount of water (20-25%) was added to the mixture to give a mix consistency that allowed formation of approximately spherical pellets with a 12-15 mm diameter.

The overall experiment comprised three major stages: sintering behavior, expanding capacity, and aggregate property. The formed pellets were dried at 105℃ in an oven for 24 hours prior to firing in an electric laboratory kiln. Firing of the synthetic aggregate consisted of presintering and sintering. The main apparatus used in this research is a self-designed electric laboratory kiln, which is programmable control and has two chambers. The dried pellets were placed in the preheating chamber of the kiln, on an alumina basement, and heated at target temperatures for different duration. Then the preheated pellets were placed in sintering chamber of the kiln and heated at desired maximum temperatures for different duration, then quenched in air.

2.4 Methods

The characteristics of the produced aggregates were determined, including particle density, water absorption, bloating ratio, and loss of ignition.

The particle density of the sintered aggregate pellets can be determined using Archimedes Principle (Neville 1994)

$$\rho_p = \frac{m_{dry}}{m_{sat} - m_{imm}} \tag{1}$$

where ρ_p = particle density; m_{dry} = dry mass; m_{imm} = immersed mass; and m_{sat} = 24-h saturated surface-dry mass.

The water absorption of the sintered aggregate pellets was determined by immersing them in water for 24 hours and was calculated from

$$Waterabsoption = \frac{m_{sat} - m_{dry}}{m_{dry}} \times 100\% \tag{2}$$

The bloating ratio was defined as the ratio of the volume of the fired pellet to the volume of the unfired pellet and was computed as

$$\text{Bloating ratio} = \frac{V_a}{V_p} \times 100\% \tag{3}$$

where V_p = initial volume of the green pellet; V_a = volume of the sintered aggregate pellet.

The loss of ignition of the dried pellet after firing was the loss in mass and was expressed as a percentage of the total initial mass.

2.5 Data analysis

In order to evaluate the influence of each selected factor on the quality characteristic being investigated, the signal to noise ratio (*S*/*N* ratio) for each control factor had to be calculated (Taguchi 2005). The *S*/*N* ratio is computed from the Mean Squared Deviation (*MSD*) (Roy 2001). In this study, the observed values of particle density, water absorption, and loss of ignition were set to minimum, while the observed values of bloating ratio were set to maximum. Thus, the *S*/*N* ratio was chosen according to the-smaller-the-better criterion or the-larger-the-better quality characteristics. In other words, the aim of any experiment is to determine the highest possible *S*/*N*

ratio for the result. If the *S*/*N* ratio (η) for the-smaller-the-better target for all the responses is expressed in decibel (dB) units, it can be defined by a logarithmic based on the *MSD* around the target value as (Roy 1990)

$$\eta = -10 \times \log_{10}(\mathrm{MSD}) = -10 \times \log_{10}\left(\sum_{i=1}^{n} y_i^2 \Big/ n \right) \tag{4}$$

where n is the number of repetitions or observations and y_i is the observed data. In the case of the-larger-the-better target, the *S*/*N* ratio (η) is generally derived from the reciprocal of its quality characteristics value as (Roy 1990)

$$\eta = -10 \times \log_{10}(\mathrm{MSD}) = -10 \times \log_{10}\left(\sum_{i=1}^{n} 1/y_i^2 \Big/ n \right) \tag{5}$$

On the other hands, the optimization of the observed values was determined by a statistical analysis of variance (ANOVA). The total sum of square deviation (SS_T) from the *S*/*N* ratio can be calculated as (Taguchi 1987, Roy 1990, Roy 2001, Taguchi 2005)

$$\mathrm{SS}_T = \sum_{i=1}^{n} (\eta_i - \eta_m)^2 \tag{6}$$

where n is the number of experiments in the orthogonal array; η_i is the mean *S*/*N* ratio for the i^{th} experiment; and η_m is the grand mean of the *S*/*N* ratio. The sum of squares from the tested parameter Z (SS_Z) can be calculated as (Taguchi 1987, Roy 1990, Roy 2001, Taguchi 2005)

$$\mathrm{SS}_Z = \sum_{j=1}^{r} \frac{Z_j^2}{t} - \frac{1}{n}\left[\sum_{i=1}^{n} \eta_i \right]^2 \tag{7}$$

where Z represents one of the tested parameter; j is the level number of parameter Z; r is the number of levels of parameter Z; t is the repeating number of each level of parameter Z; and Z_j is the sum of the *S*/*N* ratio involving parameter Z and level j. The sum of squares from error parameters (SS_e) is as (Taguchi 1987, Roy 1990, Roy 2001, Taguchi 2005)

$$SS_e = SS_T - SS_F \tag{8}$$

where SS_F represents the sum of squared deviations due to each parameter.

In addition, a statistical F test was used to determine which process parameters have a significant effect on the performance characteristic. For performing the F test, the mean of square deviation (variance) due to each process parameter and error term needs to be calculated as follows (Taguchi 1987, Roy 1990, Roy 2001, Taguchi 2005)

$$MS_Z = SS_Z / df_Z \tag{9}$$

$$MS_e = SS_e / df_e \tag{10}$$

where MS_Z is the mean of square deviation due to parameter Z; df_Z is the degree of freedom of parameter Z, MS_e is the mean of square deviation due to error term; and df_e is the degree of freedom of error term; Then, the F ratio of parameter Z (F_Z) is as (Taguchi 1987, Roy 1990, Roy 2001, Taguchi 2005)

$$F_Z = MS_Z / MS_e \tag{11}$$

The corrected sum of squares (SS_Z^*) can be calculated as:

$$SS_Z^* = SS_Z - MS_e \times df_Z \tag{12}$$

The percentage contribution of parameter Z (P_Z) can be calculated as:

$$P_Z = SS_Z^* / SS_T \tag{13}$$

3. Results and discussion

Table 5 lists the experimental results for particle density, water absorption, bloating ratio, and loss of ignition of the sintered aggregate pellets as well as the corresponding *S*/*N* ratios using Eq. (4) or Eq. (5). Since the experimental design is orthogonal, it is then possible to separate out the effect of each parameter at different levels. For example, the mean *S*/*N* ratio for the cullet content at levels 1, 2, 3 and 4 can be calculated by averaging the *S*/*N* ratios for the experiments 1-4, 5-8, 9-12, and 13-16, respectively. The mean *S*/*N* ratio for each level of the other parameters can be computed in the similar manner. The influence of each selected factor on the quality characteristic being investigated is described in detail as follows.

3.1 Particle density

The particle density of an aggregate is the ratio between the mass of the particle material and the volume occupied by the individual particles. This volume includes the pores within the particle, but does not include voids between the particles. Table 5 shows that the particle density of the produced aggregate ranged between 0.57 and 2.23 g/cm^3. Moreover, the lowest value of particle density was around 0.57 g/cm^3 (Experiment Number: G9). Table 6 (the so-called response table) shows the mean *S*/*N* ratio for each level of the parameters (A-E) for particle density. In addition, Fig. 3 shows the *S*/*N* response graph for particle density. As shown in Eq. (4), the greater is the *S*/*N* ratio, the smaller is the variance of particle density around the desired (the-smaller-the-better) value. From Table 6 and Fig. 3, it can be seen that the preheat temperature was the most important factor affecting the responses; the maximum value of response was at the lowest level of preheat temperature. Fig. 3 also indicates that the particle density decreased with the raise of sintering temperature.

The results of ANOVA for particle density are given in Table 7. The *F* values were obtained for 95% level of confidence. In addition, percentage contribution of each parameter was also calcu lated. The preheat temperature was the most significant factor that contributed maximum to the total particle density of the aggregate. The contributions from these parameters were preheat

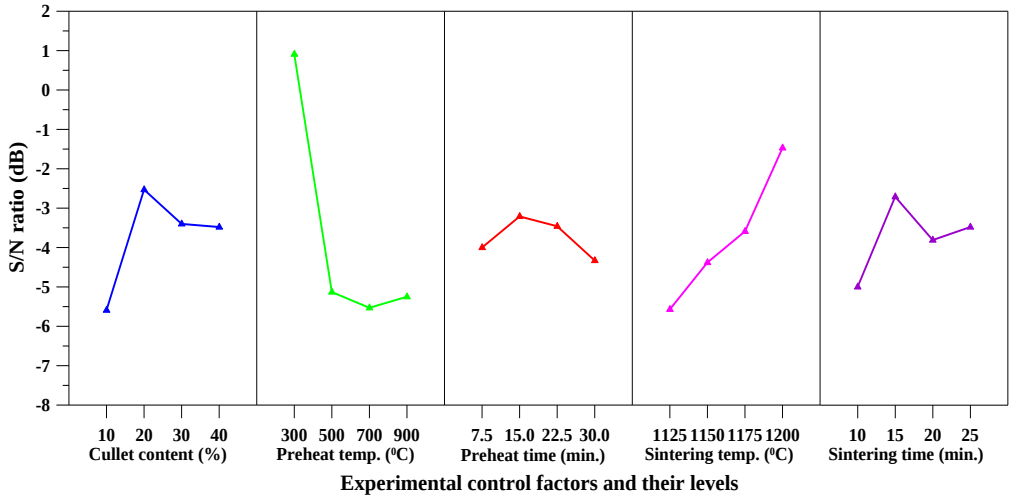

Fig. 3 S/N response graph for particle density

Table 5 Experimental results and S/N ratio

Experiment Number	Experimental results				*S/N* ratio (dB)			
	Particle density (g/cm^3)	Water absorption (%)	Bloating ratio (%)	LOI (%)	Particle density	Water absorption	Bloating ratio	LOI
G1	1.63	13.6	105.10	6.70	-4.24	-22.67	40.43	-16.52
G2	2.00	5.6	85.70	6.40	-6.02	-14.96	38.66	-16.12
G3	2.23	0.6	76.90	6.70	-6.97	4.44	37.72	-16.52
G4	1.80	0.8	95.40	5.60	-5.11	1.94	39.59	-14.96
G5	0.70	3.3	249.50	5.70	3.10	-10.37	47.94	-15.12
G6	1.25	1.5	140.20	6.10	-1.94	-3.52	42.93	-15.71
G7	1.92	10.0	90.90	4.90	-5.67	-20.00	39.17	-13.80
G8	1.91	9.6	91.40	5.00	-5.62	-19.65	39.22	-13.98
G9	0.57	4.0	310.30	5.40	4.88	-12.04	49.84	-14.65
G10	2.10	1.4	85.10	5.00	-6.44	-2.92	38.60	-13.98
G11	1.95	0.6	91.60	5.20	-5.80	4.44	39.24	-14.32
G12	2.05	4.6	87.10	4.70	-6.24	-13.26	38.80	-13.44
G13	1.01	1.2	176.80	4.60	-0.09	-1.58	44.95	-13.26
G14	2.02	1.0	88.60	4.00	-6.11	0.00	38.95	-12.04
G15	1.53	0.3	116.70	4.30	-3.69	10.46	41.34	-12.67
G16	1.59	0.2	112.40	4.30	-4.03	13.98	41.02	-12.67

Table 6 *S*/*N* response table for particle density

Parameter	Mean *S*/*N* ratio (η, Unit: dB)				Delta	Rank
	Level 1	Level 2	Level 3	Level 4	(Max. η – Min. η)	
Cullet content, A (%)	-5.59	-2.53	-3.40	-3.48	3.06	3
Preheat temperature, B (°C)	0.91	-5.13	-5.53	-5.25	6.44	1
Preheat time, C (min.)	-4.00	-3.21	-3.46	-4.33	1.12	5
Sintering temperature, D (°C)	-5.57	-4.38	-3.59	-1.47	4.10	2
Sintering time, E (min.)	-5.00	-2.71	-3.81	-3.48	2.29	4

Table 7 Analysis of variance and *F* test for particle density

Parameter	Sum of square (SS_Z)	Degree of freedom	Variance (MS_Z)	*F* value (F_Z)	$F_{0.05;3,3}$	Percentage contribution (P_Z)	Note
Cullet content, A (%)	20.18	3	6.73	6.53	9.28	9.18	Subsignificant
Preheat temperature, B (°C)	116.21	3	38.74	37.64	9.28	60.77	Significant
Preheat time, C (min.)	3.09	3	1.03	1.00	9.28	8.29	
Sintering temperature, D (°C)	35.76	3	11.92	11.58	9.28	17.55	Significant
Sintering time, E (min.)	10.91	3	3.64	3.53	9.28	4.20	
All other/Error	3.09	3	1.03				
Totall	186.15	15	62.05			100	

temperature (60.77%), sintering temperature (17.55%), cullet content (9.18%) and sintering time (4.2%). Thus, based on the *S*/*N* ratio and ANOVA analyses, the optimal combination of parameters and their levels for achieving minimum particle density is $A_2B_1C_2D_4E_2$, i.e. cullet content at level 2, preheat temperature at level 1, sintering temperature at level 2, sintering temperature at level 4, and sintering time at level 2.

3.2 Water absorption

In concrete technology, water absorption of aggregates is a measure of the total pore volume accessible to water. Rate of absorption is unique to each LWA, and is dependent on the characteristics of pore size, continuity, and distribution, particularly for those pores close to the surface. Table 5 shows that the water absorption of the produced aggregate ranged between 0.2% and 13.6%. Furthermore, some aggregates are impervious to water (water absorption below 1%). Especially, the lowest value of water absorption was around 0.2% and was obtained with sample G16. Table 8 shows the mean *S*/*N* ratio for each level of the parameters for water absorption. In addition, Fig. 4 shows the *S*/*N* response graph for water absorption. It is evident from Table 8 and Fig. 4 that the cullet content was the most critical factor affecting the water absorption; the maximum value of response was at the highest level of cullet content. Fig. 4 also indicates that the

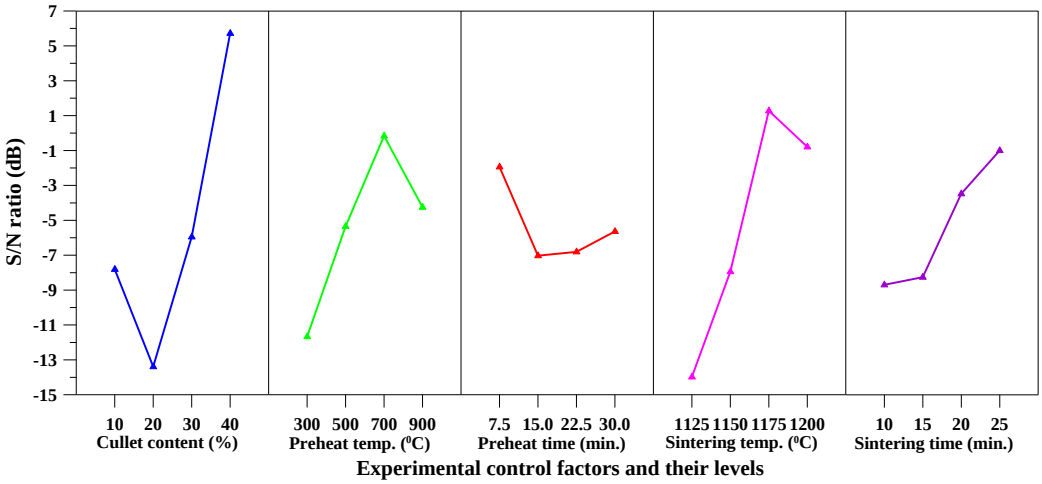

Fig. 4 S/N response graph for water absorption

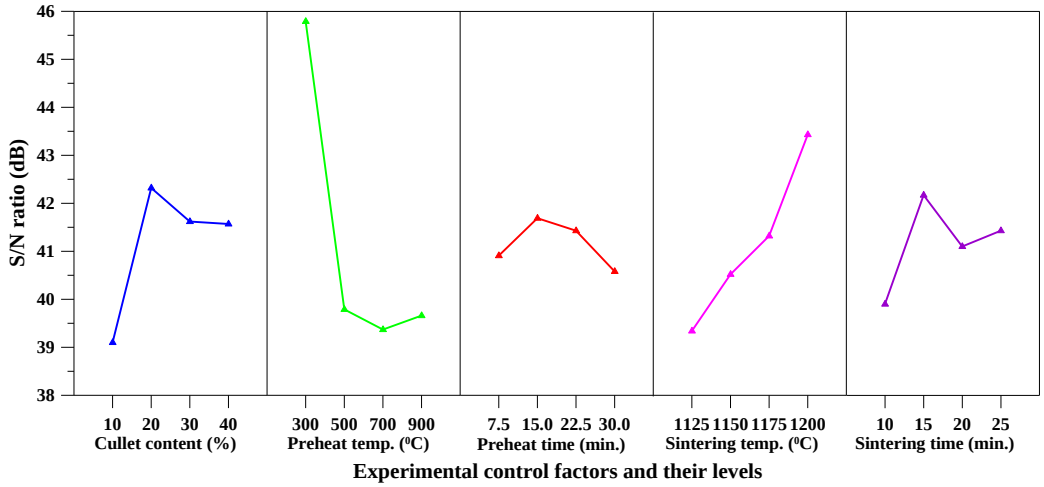

Fig. 5 S/N response graph for bloating ratio

Table 8 *S*/*N* response table for water absorption

Parameter	Mean *S*/*N* ratio (η, Unit: dB)				Delta	Rank
	Level 1	Level 2	Level 3	Level 4	(Max. η – Min. η)	
Cullet content, A (%)	-7.81	-13.39	-5.95	5.72	19.11	1
Preheat temperature, B (°C)	-11.67	-5.35	-0.16	-4.25	11.51	3
Preheat time, C (min.)	-1.94	-7.03	-6.81	-5.64	5.09	5
Sintering temperature, D (°C)	-13.98	-7.94	1.28	-0.79	15.26	2
Sintering time, E (min.)	-8.70	-8.26	-3.48	-1.00	7.70	4

Table 9 Analysis of variance and *F* test for water absorption

Parameter	Sum of square (SS_Z)	Degree of freedom	Variance (MS_Z)	*F* value (F_Z)	$F_{0.05;3,3}$	Percentage contribution (P_Z)	Note
Cullet content, A (%)	773.51	3	257.84	11.61	9.28	37.92	Significant
Preheat temperature, B (°C)	271.92	3	90.64	4.08	9.28	11.01	Significant
Preheat time, C (min.)	66.63	3	22.21	1.00	9.28	17.87	Significant
Sintering temperature, D (°C)	583.80	3	194.60	8.76	9.28	27.74	Significant
Sintering time, E (min.)	168.26	3	56.09	2.53	9.28	5.45	Subsignific ant
All other/Error	66.63	3	22.21				
Totall	1864.12	15	621.37			100.00	

water absorption decreased with the raise of sintering time.

The results of ANOVA for water absorption are given in Table 9. As can be clearly seen from Table 9, the preheat temperature was the most significant factor that contributed maximum to the total water absorption of the aggregate. The contributions from these parameters were cullet content (37.92%), sintering temperature (27.74%), preheat time (17.87%), and preheat temperature (11.01%). Therefore, based on the *S*/*N* ratio and ANOVA analyses, the optimal combination of parameters and their levels for achieving minimum water absorption is $A_4B_3C_1D_3E_4$, namely cullet content at level 4, preheat temperature at level 3, sintering temperature at level 1, sintering temperature at level 3, and sintering time at level 4.

3.3 Bloating ratio

When the light-weighting feature is a major consideration, the thermal bloating effect is a critical factor to be considered. In the study, a bloatability assessment was carried to examine the bloating characteristics of various mixes and firing conditions. Table 5 shows that the bloating ratio of the produced aggregate ranged between 76.9% and 310.3%. In other words, the largest value of bloating ratio was around 310.3% and was obtained with sample G9. Table 10 shows the mean *S*/*N* ratio for each level of the parameters for bloating ratio. Besides, Fig. 5 shows the *S*/*N* response graph for bloating ratio. From Table 10 and Fig. 5, it can be seen that the preheat temperature was the most important factor affecting the bloatability; the maximum value of response was at the lowest level of preheat temperature. Fig. 5 also indicates that the bloating ratio increased with the raise of sintering temperature.

The results of ANOVA for bloating ratio are given in Table 11. The preheat temperature was the most significant factor that contributed maximum to the total bloating ratio of the aggregate. The contributions from these parameters were preheat temperature (59.56%), sintering temperature (17.28%), cullet content (11.04%), and sintering time (4.11%). As a result, according to the results of the *S*/*N* ratio and ANOVA analyses, the optimal combination of parameters and their levels for

Table 10 *S*/*N* response table for bloating ratio

Parameter	Mean *S*/*N* ratio (η, Unit: dB)				Delta	Rank
	Level 1	Level 2	Level 3	Level 4	(Max. η – Min. η)	
Cullet content, A (%)	39.10	42.32	41.62	41.57	3.22	3
Preheat temperature, B (°C)	45.79	39.79	39.37	39.66	6.42	1
Preheat time, C (min.)	40.91	41.69	41.43	40.58	1.11	5
Sintering temperature, D (°C)	39.34	40.52	41.32	43.43	4.09	2
Sintering time, E (min.)	39.90	42.17	41.10	41.43	2.27	4

Table 11 Analysis of variance and *F* test for bloating ratio

Parameter	Sum of square (SS_Z)	Degree of freedom	Variance (MS_Z)	*F* value (F_Z)	$F_{0.05;3,3}$	Percentage contribution (P_Z)	Note
Cullet content, A (%)	23.81	3	7.94	7.90	9.28	11.04	Significant
Preheat temperature, B (°C)	115.19	3	38.40	38.23	9.28	59.56	Significant
Preheat time, C (min.)	3.01	3	1.00	1.00	9.28	8.00	Subsignificant
Sintering temperature, D (°C)	35.57	3	11.86	11.80	9.28	17.28	Significant
Sintering time, E (min.)	10.76	3	3.59	3.57	9.28	4.11	Subsignificant
All other/Error	3.01	3	1.00				
Totall	188.34	15	62.78			100.00	

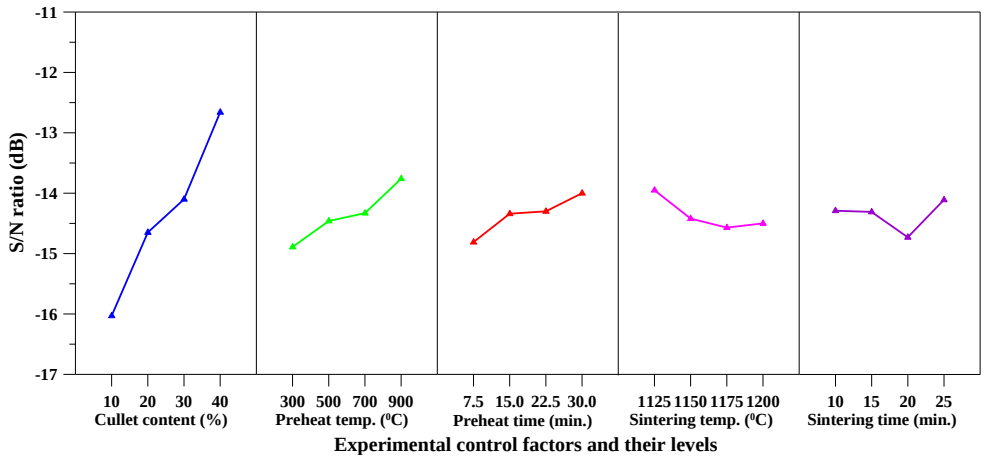

Fig. 6 *S*/*N* response graph for loss of ignition

achieving maximum bloating ratio is $A_2B_1C_2D_4E_2$, i.e., cullet content at level 2, preheat temperature at level 1, sintering temperature at level 2, sintering temperature at level 4, and sintering time at level 2.

3.4 Loss of ignition

During the process of sintering dried pellets into lightweight aggregates, mass loss occurred, probably due to water evaporation, high temperature oxidization of organic matters, decomposition of inorganic salts, etc. The mass loss percentage was defined as the ignition loss. Table 5 shows that the loss of ignition of the produced aggregate ranged between 4.0% and 6.7%. Moreover, the lowest value of loss of ignition was around 4.0% and was obtained with sample G14. Table 12 shows the mean *S*/*N* ratio for each level of the parameters for loss of ignition. In addition, Fig. 6 shows the *S*/*N* response graph for loss of ignition. From Table 12 and Fig. 6, it can

Table 12 *S*/*N* response table for loss of ignition

Parameter	Mean *S*/*N* ratio (η, Unit: dB)				Delta	Rank
	Level 1	Level 2	Level 3	Level 4	(Max. η – Min. η)	
Cullet content, A (%)	-16.03	-14.65	-14.10	-12.66	3.37	1
Preheat temperature, B (°C)	-14.89	-14.46	-14.33	-13.76	1.13	2
Preheat time, C (min.)	-14.81	-14.34	-14.30	-14.00	0.81	3
Sintering temperature, D (°C)	-13.95	-14.42	-14.57	-14.50	0.62	4
Sintering time, E (min.)	-14.29	-14.31	-14.73	-14.11	0.62	4

Table 13 Analysis of variance and *F* test for loss of ignition

Parameter	Sum of square (SS_Z)	Degree of freedom	Variance (MS_Z)	*F* value (F_Z)	$F_{0.05;3,3}$	Percentage Contribution (P_Z)	Note
Cullet content, A (%)	23.38	3	7.79	28.15	9.28	77.64	Significant
Preheat temperature, B (°C)	2.57	3	0.86	3.10	9.28	6.00	Subsignificant
Preheat time, C (min.)	1.32	3	0.44	1.59	9.28	1.70	Subsignificant
Sintering temperature, D (°C)	0.93	3	0.31	1.12	9.28	0.36	Subsignificant
Sintering time, E (min.)	0.83	3	0.28	1.00	9.28	14.30	Significant
All other/Error	0.83	3	0.28				
Totall	29.05	15	9.68			100.00	

Table 14 Particle density and water absorption of various lightweight aggregates

Parameter	Experiment number of produced LWA				Commercial LWA	
	G6	G13	G15	G16	Norwegian Leca™ (0-4 mm)	Liapor™ 8 (4-8 mm)
Particle density (g/cm^3)	1.25	1.01	1.53	1.59	1.26	1.47
Water absorption (%)	1.5	1.2	0.3	0.2	10.4	11.5

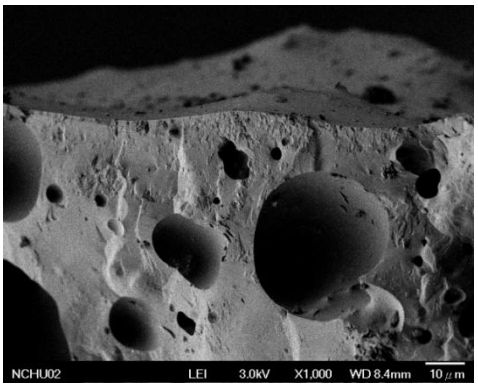

(a) Experiment number: G6

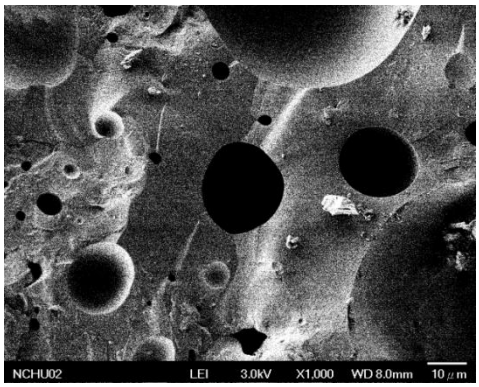

(b) Experiment number: G13

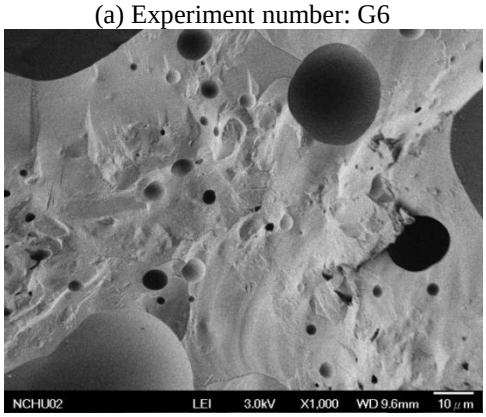

(c) Experiment number: G15

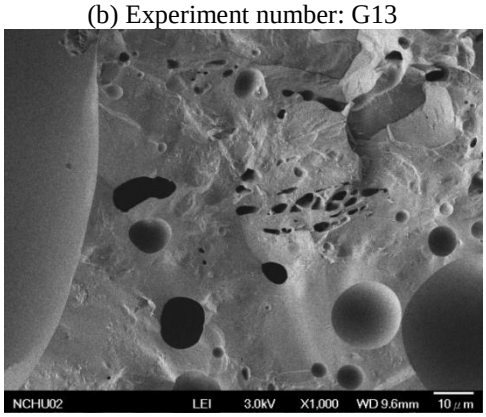

(d) Experiment number: G16

Fig. 7 The internal cellular pore system of the sintered LWA

be seen that the cullet content was the most significant factor in controlling ignition loss; the maximum value of response was at the highest level of cullet content. Fig. 6 also indicates that the loss of ignition decreased with the raise of cullet content, preheat temperature and preheat time.

The results of ANOVA for loss of ignition are given in Table 13. The cullet content was the most significant factor that contributed maximum to the total loss of ignition of the aggregate. The contributions from these parameters were cullet content (77.64%), preheat temperature (6.0%), preheat time (1.7%), and sintering temperature (0.36%). Accordingly, based on the *S*/*N* ratio and

ANOVA analyses, the optimal combination of parameters and their levels for achieving minimum loss of ignition is $A_4B_4C_4D_1E_4$, that is to say, cullet content at level 4, preheat temperature at level 4, sintering temperature at level 4, sintering temperature at level 1, and sintering time at level 4.

3.5 Discussion

Typical scanning electron microscope (SEM) micrographs of experimental combination G6, G13, G15 and G16 are shown in Fig. 7. SEM micrographs show a well-formed, dense matrix material that contains a significant volume of isolated approximately spherical porosity. These pores appear to be predominantly in the 1–15 μm diameter range, although there is evidence of some much larger pores. On the other hand, the particle density and water absorption of experimental combination G6, G13, G15 and G16 were compared with those of commercially available LWAs, i.e., Norwegian Leca^{TM} (0-4 mm) and Liapor^{TM} 8 (4-8 mm). Table 14 shows that the particle density G6 and G13 is lower than those of Leca^{TM} and Liapor^{TM} 8. Moreover, it can be clear seen that the water absorption of G6, G13, G15 and G16 is significantly lower than those of Leca^{TM} and Liapor^{TM} 8. This is in agreement with the uniform pore structure with small isolated voids in the aggregates. As a result, it can be conclude that experimental combination G6, G13, G15 and G16 are suitable for use as high performance LWA, which has low particle density and water absorption due to a uniformly distributed system of pores.

4. Conclusions

This study has presented an application of the Taguchi optimization technique to determine process condition for producing synthetic LWA by incorporating TFT-LCD glass powder with reservoir sediments. The aggregates manufactured in a laboratory had particle densities ranging from 0.57g/cm^3 to 2.23g/cm^3 and water absorption ranging from 0.2% to 13.6%. These values are comparable to the requirements for LWA. Especially, experimental combination G6, G13, G15 and G16 are suitable for use as high performance LWA. The experimental results demonstrate that it is possible to produce high performance LWA by incorporating waste TFT-LCD glass cullet with reservoir sediments. It has different types of applications, such as high-rise buildings, concrete bridge decks, precast and prestressed concrete elements etc. Moreover, Taguchi method provides a simple, systematic, and efficient methodology for optimizing process condition of synthetic LWAs using recycled glass cullet and reservoir sediments and it significantly reduces the number of tests.

Acknowledgements

The writer greatly appreciates the authority of National Science Council, Taiwan, for financing this research work under Grant NSC 99-2622-E-230-012-CC3.

References

Bajare, D., Korjakins, A., Kazjonovs, J. and Rozenstrauha, I. (2012), "Pore structure of lightweight clay aggregate incorporate with non-metallic products coming from aluminum scrap recycling industry", *J.*

Eur. Ceramic Soc., **32**(1), 141-148.
Bernhardt, M., Tellesbø, H., Justnes, H. and Wiik, K. (2013), "Mechanical properties of lightweight aggregates", *J. Eur. Ceramic Soc.*, **33**(13-14), 2731-2743.
Chandra, S. and Berntsson, L. (2002), *Lightweight Aggregate Concrete*, Noyes Publications, New York, USA.
Cheeseman, C.R., Makinde, A. and Bethanis, S. (2005), "Properties of lightweight aggregate produced by rapid sintering of incinerator bottom ash", *Res. Conserv. Recy.*, **43**, 147-162.
Cheeseman, C.R. and Virdi, G.S. (2005), "Properties and microstructure of lightweight aggregate produced from sintered sewage sludge ash", *Res. Conserv. Recy.*, **45**, 18-30.
Chen, H.J., Wang, S.Y. and Tang, C.W. (2010), "Reuse of incineration fly ashes and reaction ashes for manufacturing lightweight aggregate", *Constr. Build. Mater.*, **24**(1), 46-55.
Chen, H.J., Yang, M.D., Tang, C.W. and Wang, S.Y. (2012), "Producing synthetic lightweight aggregate from reservoir sediments", *Constr. Build. Mater.*, **28**(1), 387-394.
Chiou, I.J., Wang, K.S., Chen, C.H. and Lin, Y.T. (2006), "Lightweight aggregate made from sewage sludge and incinerated ash", *Waste Manag.*, **26**, 1453-1461.
Chung, S.Y., Han, T.S., Yun, T.S. and Youm, K.S. (2013), "Evaluation of the anisotropy of the void distribution and the stiffness of lightweight aggregates using CT imaging", *Constr. Build. Mater.*, **48**, 998-1008.
Doel, A. (2007), *Lightweight aggregates for use in concrete*, Concrete (London), **41**(7), 36-37.
Donatello, S. and Cheeseman, C.R. (2013), "Recycling and recovery routes for incinerated sewage sludge ash (ISSA): A review", *Waste Manag.*, **33**(11), 2328-2340.
Ducman, V., Mladenovič, A. and Šuput, J.S. (2002), "Lightweight aggregate based on waste glass and its alkali–silica reactivity", *Cement Concrete Res.*, **32**, 223-226.
German, R.M. (1996), *Sintering theory and practice*, New York: Viley. Interscience Publication.
Huang, C.H. and Wang, S.Y. (2013), "Application of water treatment sludge in the manufacturing of lightweight aggregate", *Constr. Build. Mater.*, **43**, 174-183.
Kayali, O. (2008), "Fly ash lightweight aggregates in high performance concrete", *Constr. Build Mater*, **22**(12), 2393-2399.
Kourti, I. and Cheeseman, C.R. (2010), "Properties and microstructure of lightweight aggregate produced from lignite coal fly ash and recycled glass", *Res. Conserv. Recy.*, **54**(11), 769-775.
Liao, Y.C., Huang, C.Y. and Chen, Y.M. (2013), "Lightweight aggregates from water reservoir sediment with added sodium hydroxide", *Constr. Build. Mater.*, **46**, 79-85.
Metha, P.K. and Monteiro, P.J.M. (2006), *Concrete; Microstructure, Properties and Materials*, 3rd Edition, McGraw-Hill, New York.
Mindess, S., Young, J.F. and Darwin, D. (2003), *Concrete*, Prentice Hall.
Muellera, A., Sokolova, S.N. and Vereshagin, V.I. (2008), "Characteristics of lightweight aggregates from primary and recycled raw materials", *Constr. Build. Mater.*, **22**, 703-712.
Mun, K.J. (2007), "Development and tests of lightweight aggregate using sewage sludge for nonstructural concrete", *Constr. Build. Mater.*, **21**, 1583-1588.
Neville, A.M. (1994), *Properties of concrete*, Harlow: Longman.
Qiao, X.C., Ng, B.R., Tyrer, M. and Poon, C.S. (2008), "Cheeseman CR. Production of lightweight concrete using incinerator bottom ash", *Constr. Build. Mater.*, **22**(4), 473-480.
Riley, C.M. (1951), "Relation of chemical properties to the bloating of clays", *J. Am. Ceramic Soc.*, **30**(4), 121-128.
Roy, R.K. (1990), *A Primer on the Taguchi method*, *Competitive Manufacturing Series*, Van Nostrand Reinhold, New York.
Roy, R.K. (2001), *Design of Experiments Using the Taguchi Approach*, John Wiley & Sons, Inc.
Shon, C.S., Jung, Y.S., Saylak, D. and Mishra, S.K. (2013), "Development of synthetic aggregate using off-ASTM specification ashes", *Constr. Build. Mater.*, **38**, 700-707.
Somayaji, S. (2001), *Civil engineering materials*, 2nd ed., Prentice Hall, Upper Siddle River, New Jersey.
Taguchi, G., Chowdhury, S. and Wu, Y. (2005), *Taguchi's Quality Engineering Handbook*, New York, Wiley.

Taguchi, G. (1987), *Introduction to quality engineering: designing quality into products and processes*, Asian Productivity Organization, Tokyo, Japan.
Tang, C.W., Chen, H.J., Wang, S.Y. and Spaulding, J. (2011), "Production of synthetic lightweight aggregate using reservoir sediments for concrete and masonry", *Cement Concrete Compos.*, **33**(2), 292-300.
Wainwright, P.J. and Cresswell, D.J.F. (2001), "Synthetic aggregate from combustion ashes using an innovative rotary kiln", *Waste Manag.*, **21**, 241-246.
Yaghi, N. and Hartikainen, H. (2013), "Enhancement of phosphorus sorption onto light expanded clay aggregates by means of aluminum and iron oxide coatings", *Chemosphere*, **93**(9), 1879-1886.

CC